Spring 5-2-2021

Characterization of Mechanical Responses of Helical Antenna for Satellite Communications

Scott Chumley

Characterization of Mechanical Response of Helical Antenna for Satellite Communication

By Scott Chumley

A thesis submitted to the faculty of The University of Mississippi in partial fulfillment of the requirements of the Sally McDonnel Barksdale Honors College

Oxford
May 2021

Approved by

Advisor: Dr. Joel Mobley

Reader: Dr. Cecille Labuda

Reader: Dr. Craig Hickey

TABLE OF CONTENTS

ABSTRACT

The purpose of this work was to identify and analyze the vibrational modes of a helical structure to model the vibrational characteristics of an L-band helical antenna for satellite communications. This project focused on the vibrational modes between 1 and 50 Hz. Using COMSOL Multiphysics finite element modeling of helices were performed to predict mode shapes and frequencies to compare with both continuous wave (CW) and impulsive measurements. In the initial phase of the experimental work, five helical samples were constructed and evaluated. In the second phase of the study, one sample was chosen for more detailed quantitative measurements. In the CW measurements, frequency sweeps between 1 and 50 Hz were conducted where excitations and measurements of both longitudinal and transverse responses were performed. The impulsive study utilized both the transverse and longitudinal excitations and measurements of both longitudinal and transverse responses were performed. The data were recorded under LabVIEW control and analyzed in MATLAB. The data show the predicted modes from the finite element modeling (FEM) study offered similar results to the experimental studies with differences ranging from 0.1 to 10%.

LIST OF FIGURES

LIST OF TABLES

INTRODUCTION

The purpose of this thesis project was to identify and analyze the vibrational modes of helical structures that model an L-band helical antenna used for satellite communications to be deployed in low-earth orbit (LEO). According to NASA, LEO is defined by the first 100 to 600 miles of space. The orbital periods associated with LEO average about 90 minutes which corresponds to a rate of 16 orbits a day. This type of orbit is the easiest to get to and stay in, making it extremely common in satellite imaging, and communications. One example of an LEO object is the International Space Station (ISS) (Wild 2017). Unlike Geostationary Equatorial Orbit (GEO), LEO is not limited to equatorial orbits, but is free to orbit the Earth along any path. The satellites of interest in this project will facilitate ground-to-ground communications.

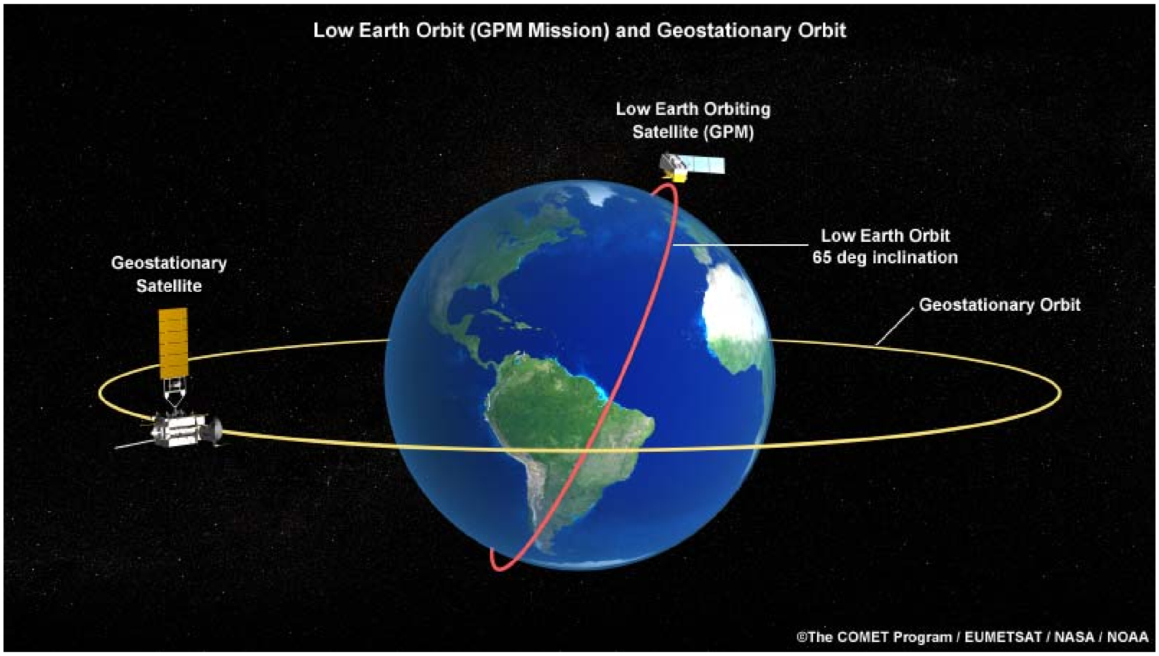

Figure 1: Image depicting difference between LEO and GEO satellite orbits. Taken from SatFC-J: Satellite Foundational Course for JPSS

The overall goal of this project was to analyze and characterize the vibrational modes of a helical antenna in order to identify each of the modes and ultimately determine an effective damping method. As a satellite in LEO moves around the Earth, there are several stresses that could induce vibrations in the antenna. Because the satellite is moving in an angular orbit rather than a straight line, the antenna will be subject to some shear stress at the tip of the antenna which could stimulate vibration. Not only is its motion a stressor but in equatorial orbit, the satellite will be subject to the radiant energy from the sun which can give rise to dramatic heating and cooling cycles as the satellite passes in and out of the shadow of the Earth.

The work reported here focused on identifying the vibrational modes of a helix between 1 and 50 Hz in order to determine the modal frequencies and its responses in this range. This will assist in determining an effective way to damp the helix, by either covering it in a flexible sheath, by running a boom down the axis, or by other methods.

Figure 2: Each Helical sample labeled from 1 (Far left) to 5 (far right)

	Sample 1	***Sample 2***	***Sample 3***	***Sample 4***	***Sample 5***
Number of Turns	12	16	22	16	17
Radius of Coil (m)	0.063	0.03325	0.03505	0.0525	0.04605
Radius of Wire (m)	0.0016	0.0016	0.0012	.00335	0.0016
Length (m)	0.49	0.485	0.56	1.3	0.71
Axial Pitch (m)	0.0408	0.0303	0.0254	0.08125	0.0417

Table 1: Specifications of size, length and makeup of each constructed sample

In the initial phase of the project, five helical elements were characterized, Table 1 shows the specifications of each helical sample and they are shown in Figure 2. Each sample was constructed by the machine shop in the National Center of Physical Acoustics

(NCPA) using spring steel. The project consisted of three stages. The first stage was the numerical simulations of the vibrational characterization of helical structures using FEM. The second phase involved the semi-quantitative evaluation of the five helical samples. The third phase involved a complete quantitative evaluation of a single sample.

THEORY

Damped Harmonic Oscillator

This project focuses on a damped harmonic oscillator system. In this work, we consider two methods of excitation: continuous wave and impulsive.

For the CW case, the driving force can be described as $Fe^{i\omega t}$ where $\omega = 2\pi f$ and f is the controlled frequency with units in Hz. The impulsive case has a force that can be described as $F\delta(t)$ where $\delta(t)$ is the delta function. The two solutions are Fourier transforms of each other. The solution to the $Fe^{i\omega t}$ drive can be called the spectral response, while the transient response relates to the impulse solution. These responses can also be called the frequency domain, in the case of CW, and the time domain, in the impulsive case, solutions.

The damped harmonic oscillator equations of motion can be derived from Newton's second law.

$$\Sigma F = m\frac{d^2x}{dt^2} \tag{1}$$

In the case of a damped harmonic oscillator this becomes

$$m\frac{d^2x}{dt^2} = -kx - b\frac{dx}{dt} + Fe^{i\omega t} \tag{2}$$

Where kx is the restoring force and b is the damping coefficient

$$\frac{d^2x}{dt^2} = -\omega_0^2 x - 2\Gamma\frac{dx}{dt} + \frac{F}{m}e^{i\omega t} \tag{3}$$

Where $\omega_0^2 = k/m$ and $2\Gamma = b$

By rearranging the previous equation, it can be rewritten as

$$\frac{d^2x}{dt^2} + \omega_0^2 x + 2\Gamma\frac{dx}{dt} = \frac{F}{m}e^{i\omega t} \tag{4}$$

Assuming the solution holds the form $\tilde{A}e^{i\omega t}$, the equation of motion becomes

$$(-\omega^2 + i2\Gamma\omega + \omega_0^2)\tilde{A} = \frac{F}{m} \tag{5}$$

Through further simplification this becomes

$$\tilde{A} = \frac{F/m}{\omega_0^2 - \omega^2 + i2\Gamma\omega} \tag{6}$$

$\tilde{A}$ can be written in form of amplitude and phase as

$$\tilde{A} = Ae^{i\phi} = A(cos(\phi) + isin(\phi)) \tag{7}$$

Where A is the modulus of $\tilde{A}$. Now we can solve for A

$$A = \frac{F/m}{\sqrt{\left(\omega_0^2 - \omega^2\right)^2 + 4\Gamma^2\omega^2}} \tag{8}$$

And

$$\phi = \tan^{-1}\left(\frac{Im(\tilde{A})}{Re(\tilde{A})}\right) = \left(-\frac{2\Gamma\omega}{\omega_0^2 - \omega^2}\right) \tag{9}$$

At frequencies well below the resonance, it is clear ϕ becomes

$$\phi = \left(-\frac{2\Gamma\omega}{\omega_0^2 - \omega^2}\right) \rightarrow -\frac{2\Gamma}{\omega_0^2}\omega \tag{10}$$

In this limit ϕ looks like $tan^{-1}(0^-) = -\pi$

As resonance

$$\phi = \left(-\frac{2\Gamma\omega}{\omega_0^2 - \omega^2}\right) \rightarrow \infty \tag{11}$$

thus $\phi = \frac{\pi}{2}$

At frequencies much larger than resonance

$$\phi = \left(-\frac{2\Gamma\omega}{\omega_0^2 - \omega^2}\right) \rightarrow \frac{2\Gamma}{\omega} \tag{12}$$

As ω continues to increase the limit $\phi = tan^{-1}(0^+) = 0$

When the frequency sweeps through a resonance the phase shifts by about 180 degrees which can provide evidence for the presence of a mode even when the amplitude is significantly smaller compared to other spectral features.

If the system is excited by an impulse rather than a continuous driving force the time domain solution can be shown as

$$x(t) = \Theta(\mathrm{t})e^{-\Gamma t}\sin(\omega_d\, t) \qquad (13)$$

Where $\omega_d = \sqrt{(\omega_0^2 - \Gamma^2)}$ and $\Theta(t)$ is the unit step function.

It can be shown that the frequency domain solution $A(\omega)e^{i\phi(\omega)}$ and the time domain solution $x(t)$ are related by the Fourier transform. By knowing the transient response of the system, its spectral response can be obtained utilizing the Fourier transform. This is the basis for obtaining the spectra of the helix from its response to an excitation caused by an impulse.

This theory could be applied to the regions around the peaks and using fitting techniques determine Γ and ω_0 for each mode. This will be done in future work, this study was primarily concerned with locations of the mode and not the damping so Lorenztian fitting was not pursued.

METHODS

In the first phase of the project, COMSOL Multiphysics was used to simulate each of the samples using Finite Element Modeling (FEM). The model was constructed with parameters such as the length and radii following the specifications of the constructed samples (Table 1). An eigenfrequency study was run to determine the first ten modes that would characterize the helices' vibrational states. These eigenfrequencies were then compared with the results from the studies of the constructed samples. The laboratory determined modal frequencies and types through direct observations rather than with quantitative methods.

In Phases 2 and 3, a Polytec IVS-500 Laser Doppler Vibrometer (LDV) was used to measure the vibrational characteristics of the samples. This instrument uses a laser to track the vibrations of an object using the Doppler effect. The LDV tracks the changes in frequency or phase of a light beam that has been scattered by a target using two light beams referred to as a reference beam and a measurement beam. The LDV uses highly precise interferometry in which a single beam is split into the reference and measurement beam. The reference beam travels directly to a photodetector while the measurement beam is incident on the target. As the target moves along the direction of the beam the measurement beam is reflected back into the LDV. Due to the vibrations of the sample, the frequency and phase of the measurement beam is shifted. The measurement beam is then superimposed with the reference beam which reveals the Doppler shifts due to the vibrations. A schematic diagram of the LDV interferometry system is provided in Figure 4.

The superimposition of the light beams creates optical interference where the intensity of this new light beam is found not by the sum of the two beams intensity but rather by the formula

$$I_{tot} = I_1 + I_2 + 2\sqrt{I_1 I_2}\cos[\frac{2\pi(r_1 - r_2)}{\lambda}] \quad (14)$$

Where I_1 and I_2 are the intensities of the measurement and reference beams, r_1 and r_2 are the optical paths of the measurement and reference beams, respectively, and λ is the wavelength of the emitted beam. Signal processing is then used to determine the vibrational velocity and displacement of the target.

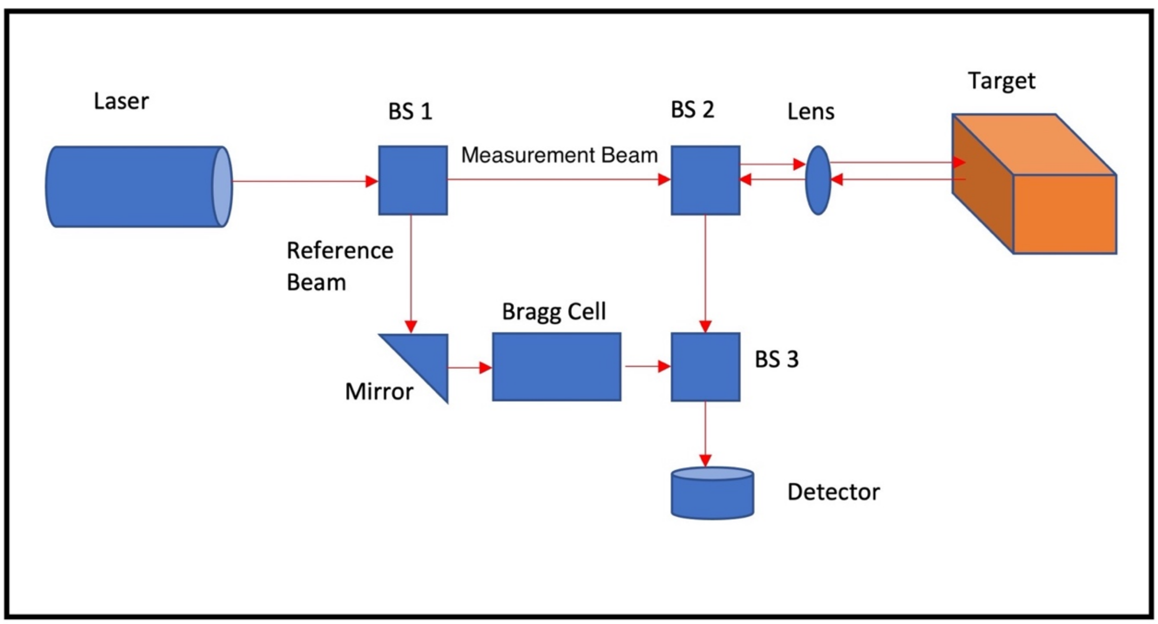

Figure 3: Diagram of the LDV interferometry system. BS stands for beam-splitter.

In order to track the motion of the helix, a reflective tab was used as a target for the LDV since the coils along the helix were not sufficiently large to get a reliable signal. The tab was attached to a coil in order to measure its motion, then it was moved to an adjacent coil. This was repeated until data from each coil along the helix had been acquired. In this manner, a set of spectra representing the entire helix was captured. The tab was made to be lightweight in order to minimize its impact on the motion of a coil.

Phase 1 of the study involved the development of finite element models of the five helical samples to numerically predict the mode shapes and frequencies. These numerical simulations were carried out using an eigenfrequency study of each of the models which were constructed using specifications of its manufactured counterpart. In this work, only sample 2 is referenced.

Phase 2 of the study consisted of the experimental identification of modes for all five samples for comparison with the numerical results. This involved mostly visual testing with some tracking of the modes by use of the LDV. In these studies, the system is excited by continuous waves using a shaker and scanned through frequencies from 1 to 20 Hz in order to visually gain an understanding of how each sample reacted. One of the samples (Sample 2) was selected for more extensive quantitative characterization in Phase 3 in which we scanned through 1 to 50 Hz. Sample 2 was selected from the five shown in Figure 2 (also see Table 1).

Two simulation studies were conducted on this sample, the first being a fixed end and free end boundary condition, meaning one end of the helix was fixed to a boundary while the other was free to move without restraint. A finite element analysis of the fixed end condition was run to get a clear idea of the frequencies and shapes of the first ten eigenmodes. The transverse modes came in pairs consisting of motion in orthogonal planes having frequencies very close to one another. This motion manifest itself in a circular swinging movement that can be seen in the experiments done in Phases 2 and 3.

Due to this motion, the FEA resulted in only 7 distinct mode shapes among the ten frequencies. The second simulation used a free-free boundary condition allowing for the sample to move freely at both ends. This simulation offered a better match to the experimental results compared to the fixed-free condition. Therefore, only the free-free simulation results will be referred to in the rest of this thesis. Similar to the fixed-free results, the free-free also exhibited a pairing of transverse modes resulting in only 7 distinct mode shapes as shown in Table 2.

Sample 2 FEM Simulation Frequency (Hz)	**Mode Shape Type**
7.867 and 7.871	Transverse Pair
16.11	Longitudinal
18.477	Torsional
19.978 and 19.989	Transverse Pair
32.008	Longitudinal
35.683 and 35.69	Transverse Pair
36.821	Torsional

Table 2: Table of FEM simulation frequencies and the mode shapes correlating to each frequency. Using free end boundary conditions

In Phase 3, the quantitative phase of the work, various stimuli and response orientations were used: Longitudinal Evaluated-Longitudinal Excited (LE-LE) Longitudinally Evaluated-Transversally Excited (LE-TE), and Transverse Evaluated-Transverse Excited (TE-TE). In each, the first term refers to the applied stimulus and the second to the type of motion that was measured. These are described below.

LE-LE

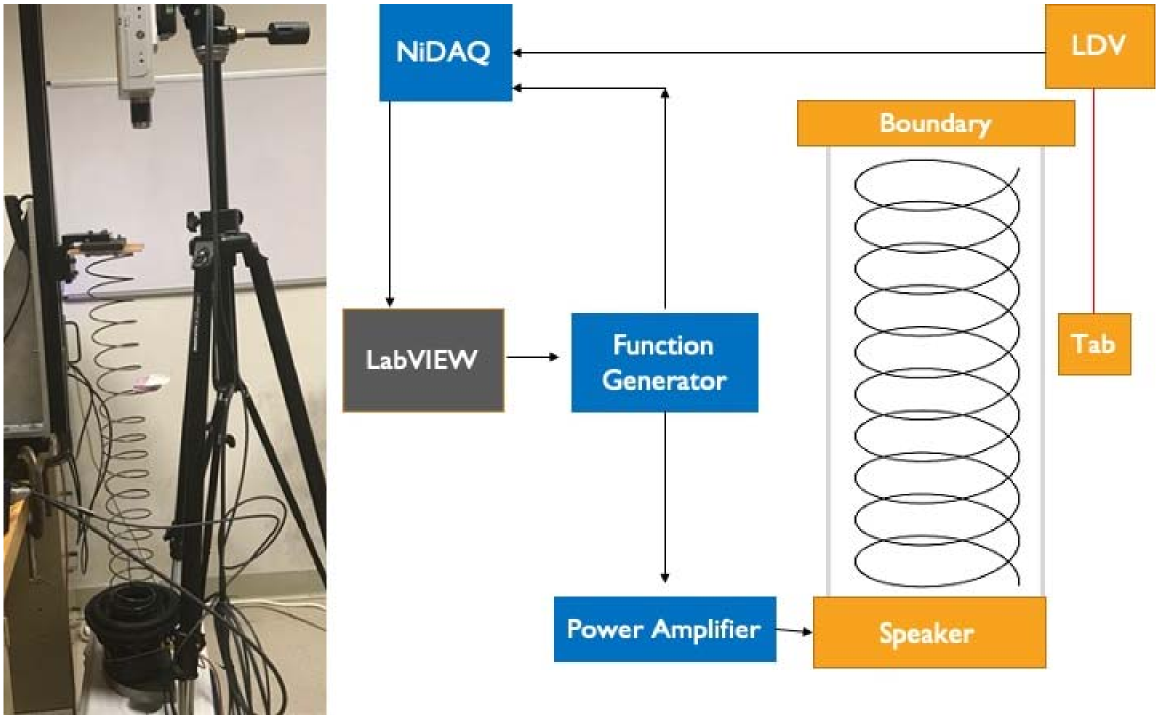

Figure 4: LE-LE Configuration

For our LE-LE configuration as depicted in Figure 4, a speaker was positioned directly underneath the helix allowing for a stimulus (CW or Impulse) appropriate to the specific study. The CW measurements consisted of a frequency sweep from 1-50 Hz, while impulsive measurements used a short a pulse. In the LE-LE case, the stimulus is applied longitudinally through the helix.

LE-TE

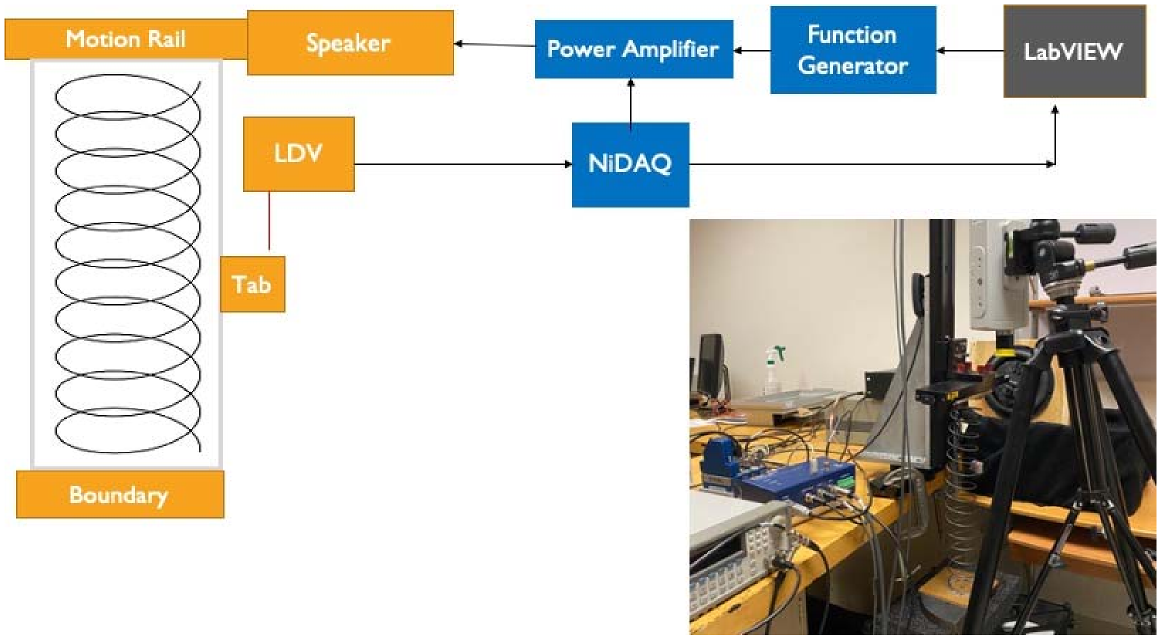

Figure 5: LE-TE Configuration

Similar to the LE-LE, the LE-TE configuration (Figure 5) provided for a longitudinal evaluation of the motion of the helix under a transverse excitation. The LDV was aligned to point down vertically to target the tab as it was moved from coil-to-coil. Instead of putting the speaker to actuate motion by direct contact, it was connected to a horizontally oriented linear motion rail that was connected to the sample. The helix was then attached to a weight at the bottommost coil to keep it in place as the speaker moved the helix transversely at its topmost coil. This configuration was not implemented until the impulse study.

TE-TE

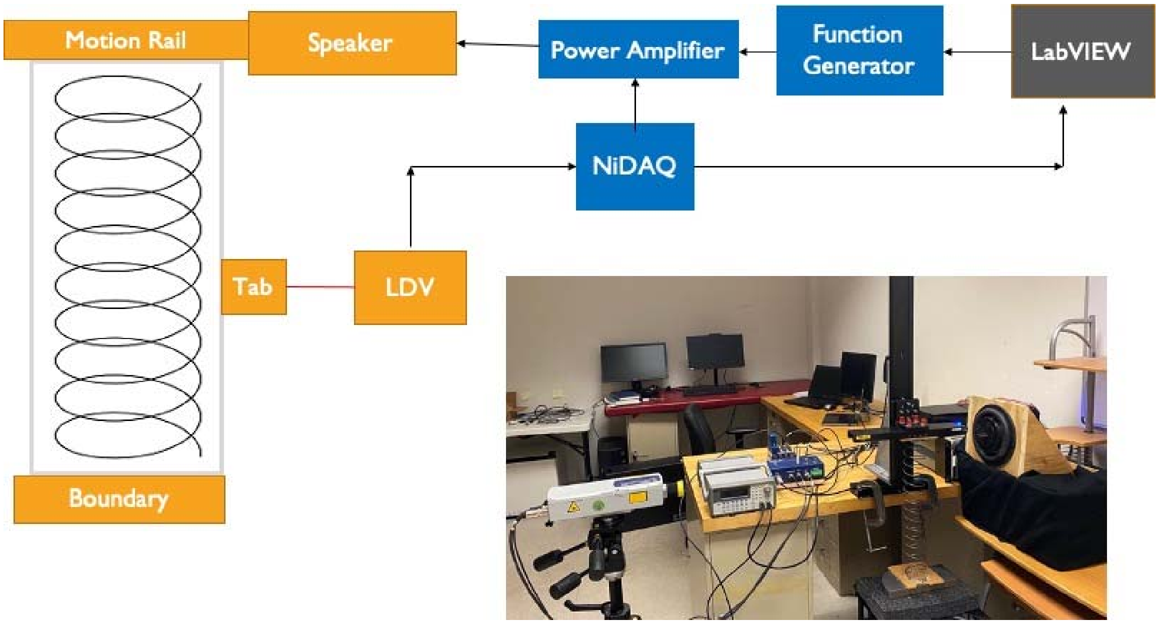

Figure 6: TE-TE Configuration

In the TE-TE configuration (Figure 6), the stimulus system and helix were configured in the same way as with the LE-TE. The LDV was positioned to target the tab oriented in a plane perpendicular relative to the helix. This allowed for the measurements of the transverse modes under transverse excitation.

During this experiment, LabVIEW and MATLAB were utilized in the signal processing and data analysis. A LabVIEW interface provided the means for running the system and controlled the master trigger for the instruments. The signal from the LDV was digitized by the NI box which downloaded the data to the computer where it was stored to a binary file. From there, MATLAB code was used to convert the binary files into a MATLAB workspace format, so that further analysis could take place. Then the data were run through the analysis code which generated a spectrum for each coil. A figure of the signal was also processed to determine whether the LDV received a signal of sufficient quality during the trial. Finally, the MATLAB workspaces taken at each of the coils were used to create a spectrum for the total helix which allowed for a visual representation of the full modal response of the helix.

The goal of taking measurements in the different orientations of the LDV and excitation methods was to check the consistency between the measurements and predictions of the modal frequencies. It is expected that the helix should exhibit the same modal frequencies no matter the orientation; however, the amplitudes may be different as certain mode shapes will be excited more in one orientation than the other. For example, in the LE-LE experiments the longitudinal mode frequencies exhibited very large peaks while the transverse modes showed much smaller peaks. It is not unexpected that in the LE-LE and TE-TE configurations that some modes do not exhibit themselves clearly or with a sufficient amplitude to even be registered. Because of this, it was important for both the LE-LE and TE-TE configurations to be examined thoroughly to identify the full spectrum.

Continuous Wave Measurements

Once the FEM was completed on Sample 2, the next step involved continuous wave measurements. During this study, only the LE-LE and TE-TE configurations were used. A frequency sweep was performed in an effort to match the simulated frequency results to the measured results. For the most part, the continuous wave experimental and simulated modal frequencies matched each other, some differing by a few Hz. In this experiment, a Model SR850 Lock-in Amplifier was used to run a frequency sweep from 1-50 Hz with the output fed to a Crown XLS1002 DriveCore power amplifier in order to match the impedance and increase the amplitude of the sinusoidal signal driving the speaker. The signal was then run into the speaker which was coupled to the sample in the two configurations described earlier. During each data acquisition, three trials were taken per coil, each moving the reflective tab down the helix one coil at a time starting from the topmost free coil and moving down the helix in a straight line ending at the last free coil at the bottom. A total of 14 coils were tracked.

By moving the reflective tab down the spring, it was possible to track the response at each coil. This was important as it made it possible to identify the mode shapes and compare the experimental observations with the predictions from the COMSOL simulations. After all the measurements were taken, the data sets were analyzed using MATLAB code to generate a plot of the amplitude vs frequency for each coil. These figures were used track the positions of different nodes and antinodes on each coil at each frequency at which modes were identified.

Impulsive Measurements

The next phase of the study involved impulsive stimuli. Here the helix was excited by a sharp impulse allowing the helix to experience a 'ring down' effect causing it to vibrate until it returns to rest. This approach is expected to generate a large number of modes simultaneously which can be individually measured using Fourier analysis.

The setup in this phase is very similar to that of the CW acquisition system. Here a function generator (Agilent 33205A 80MHz Function/Arbitrary Waveform generator) is used to generate the initial excitation pulse which is fed to a power amplifier (Crown XLS1002 DriveCore) whose output is impedance matched to the speaker. The speaker output is pulsed every 20 seconds. This interval allows time for the helix to fully ring down between excitations guaranteeing that each measurement is independent. The LDV acquires the data from the reflection from the lightweight tab. This analog data is then captured using a NiDAQ digitizer. The digitized data is then sent to the computer where the LabVIEW code writes it to a binary file. The digitizer receives three channels: the output from the function generator, the LDV signal data, and the sync output from the function generator. The impulsive study called for all three configurations (LE-LE, LE-TE, TE-TE) to be run. At each measurement point, three signals were acquired to ensure the consistency of the data. During this phase, it was desired to take data for both the orthogonal directions that the transverse modes occurred in.

RESULTS

In this section, the experimental data collected in both the CW and impulsive study will be presented and compared to the results of the COMSOL study. Figures 7-10 show each mode found in the COMSOL study. The results from the FEM simulations will be compared to the findings of the experimental studies. In each section, there will be figures showing the spectrum of the entire helix. This spectrum is a summation of the spectra of data taken at each coil. Once the entire spectrum of the helix is found, most if not all the modal frequencies will be identified. Finally, the spectra of data taken at each coil will be presented in a summary figure.

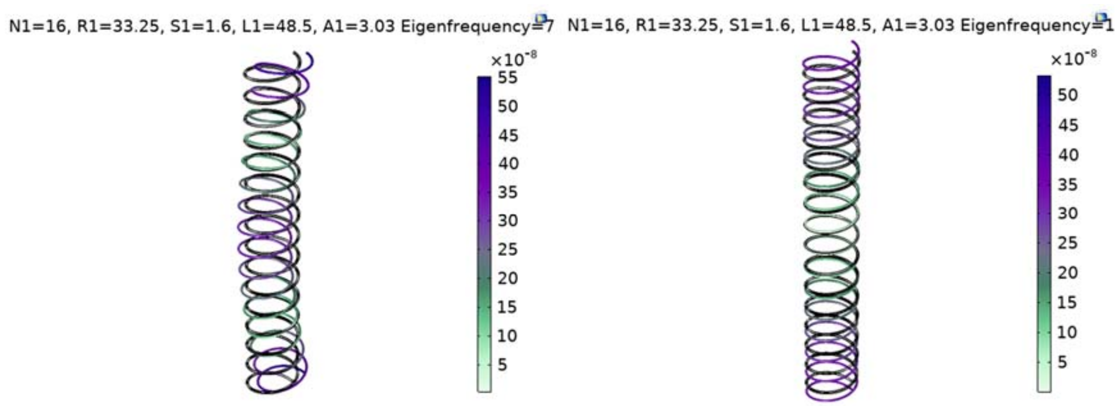

Figure 7: Image of FEM (free end boundary conditions) simulated 7.87Hz transverse pair mode (Left) and 16.11Hz Longitudinal Mode (Right)

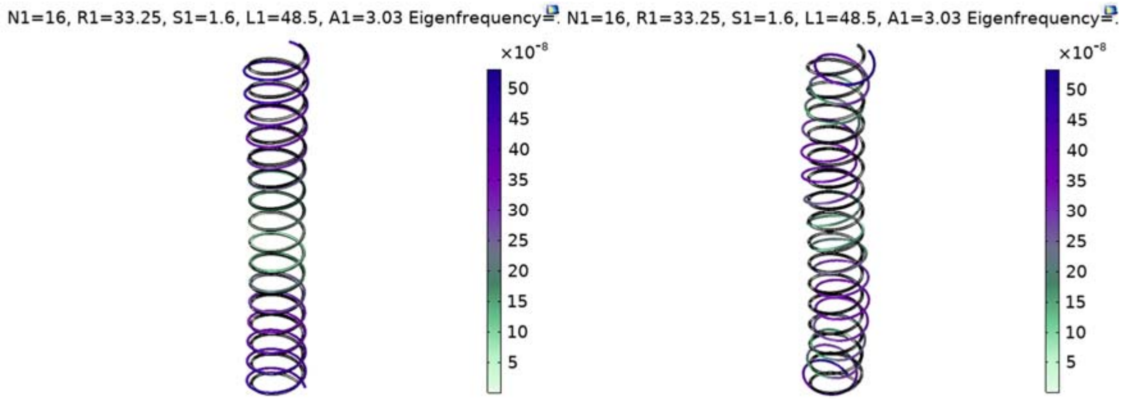

Figure 8: Image of FEM (free end boundary conditions) Simulated 18.48 Hz Torsional mode (Left) and 19.98 Hz Transverse pair mode (Right)

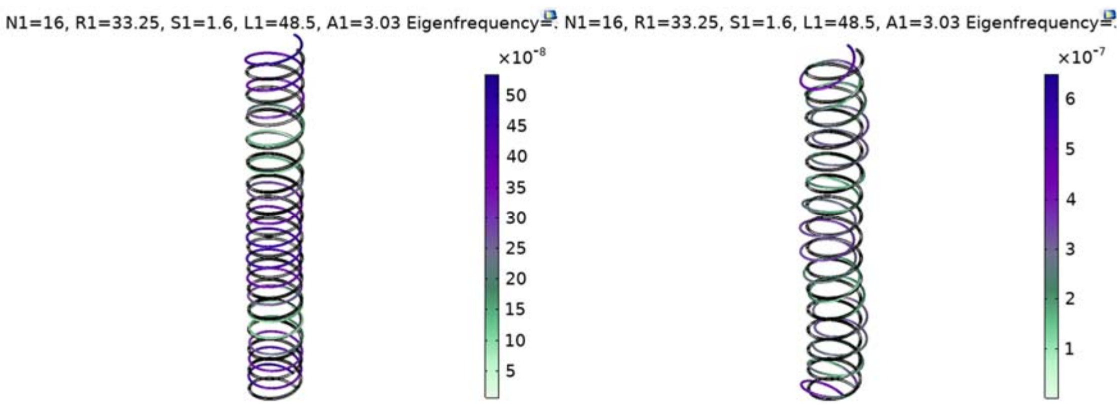

Figure 9: Image of FEM (free end boundary conditions) simulated 32.01 Hz Longitudinal mode (Left) and 35.68 Transverse pair mode (Right)

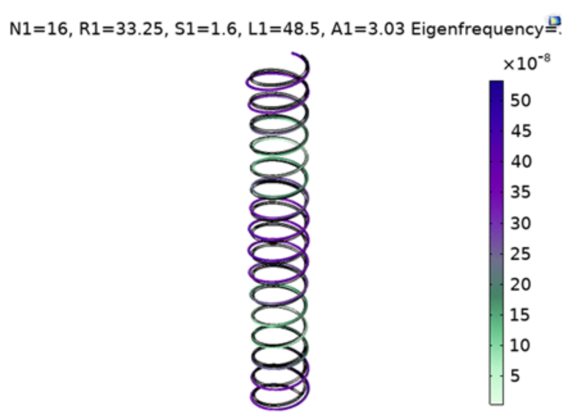

Figure 10: Image of FEM (free end boundary conditions) simulated 36.32 Hz Torsional mode

CW Results

LE-LE

Figures 11 and 12 depict the entire spectrum presented in the CW study during the LE-LE phase. As shown in Figure 11, there are two distinct peaks at 15.33 and 30.64 Hz. Referring back to Table 2, these frequencies most closely resemble the longitudinal modes at 16.11 and 32.01 Hz. The other modes can be seen in Figure 12. These amplitudes are much smaller than the longitudinal modes; however, this was expected due to the excitation and evaluation methods both being longitudinal. Smaller peaks can be seen at 8.04, 17.88, 20.00, 32.98, and 36.37 Hz. Figure 13 shows the collection of spectra taken coil by coil for the LE-LE CW study.

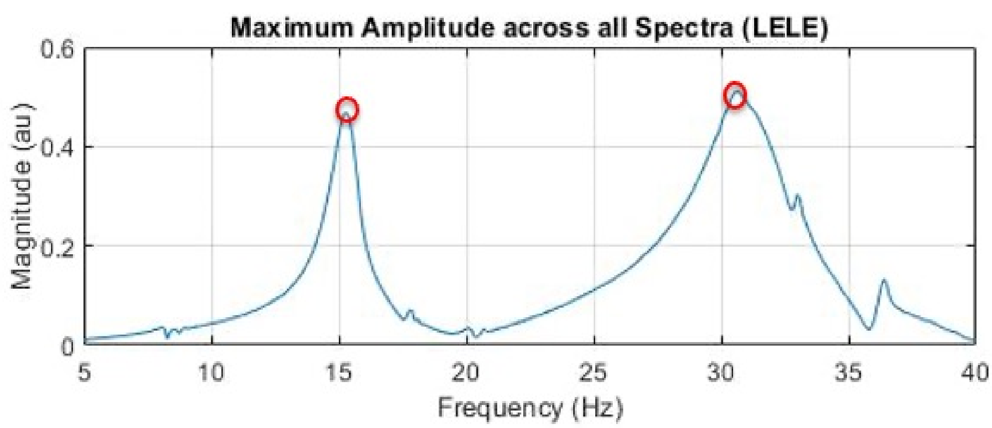

Figure 11: Helix spectrum of LE-LE CW data. Two large peaks at 15.33 and 30.64 Hz. Although the y-axis is labeled in units (au), the figure actually tracks velocity(m/s).

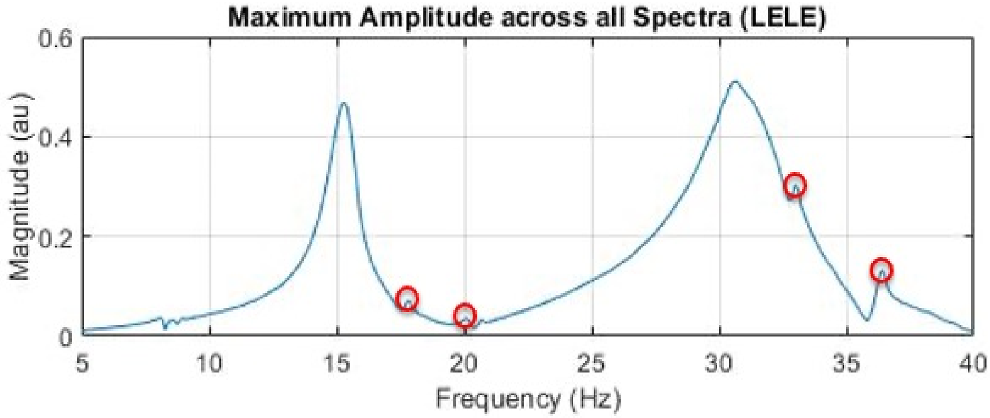

Figure 12: Helix Spectrum of LE-LE CW data. Five small peaks at 17.88, 20.00, 32.98, and 36.37 Hz. Although the y-axis is labeled in units (au), the figure actually tracks velocity(m/s).

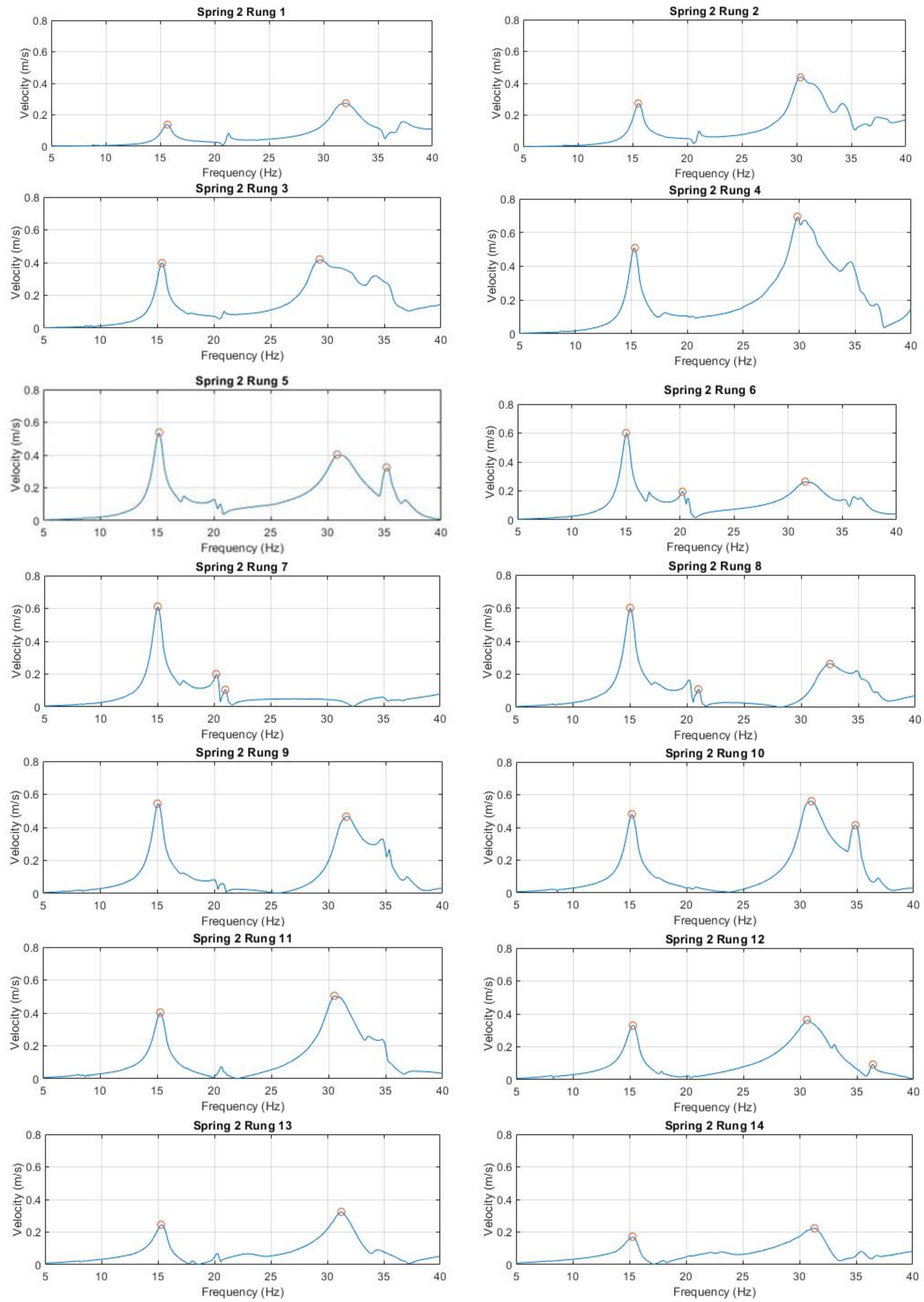

Figure 13: Spectra of data taken at each coil in CW LE-LE study

TE-TE

Figures 14 and 15 depict the full helix spectrum of the CW TE-TE study. Figure 14 shows two large peaks at the 17.88 and 33.91 Hz. These correlate to the 18.48 Hz torsional mode and the transverse pair near 35.68 Hz. Figure 15 shows much smaller peaks near 15.54, 20.00, 31.22, and 36.84 Hz. Figure 16 shows the spectra of the helix coil by coil.

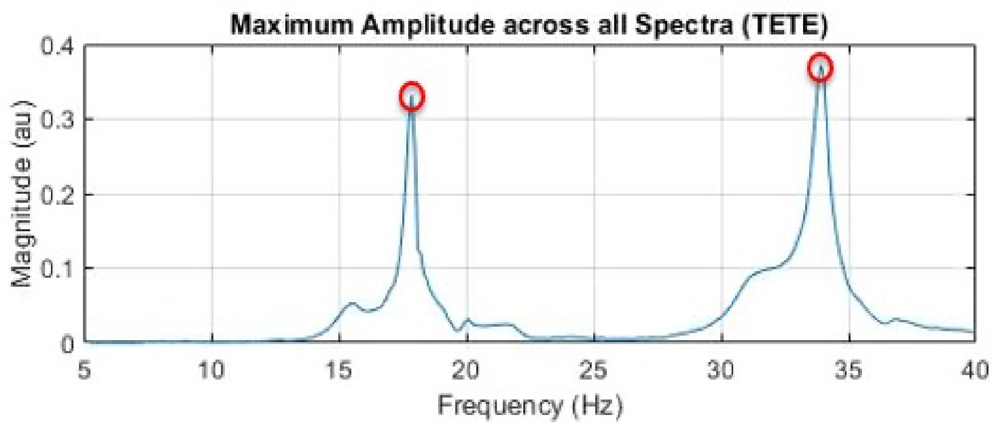

Figure 14: Helix Spectrum of TE-TE CW. Two large peaks near 17.88 and 33.91 Hz. Although the y-axis is labeled in units (au), the figure actually tracks velocity(m/s).

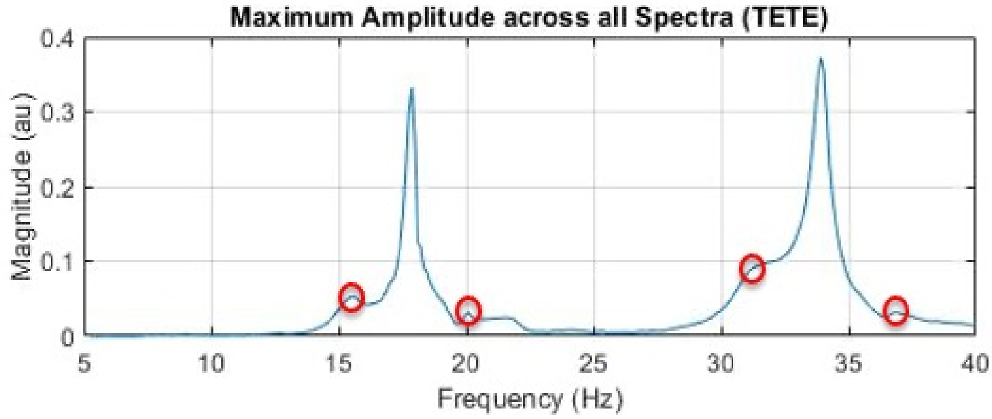

Figure 15: Helix Spectrum of TE-TE CW. Peaks at 15.54, 20, 31.22, 36.84 Hz. Although the y-axis is labeled in units (au), the figure actually tracks velocity(m/s).

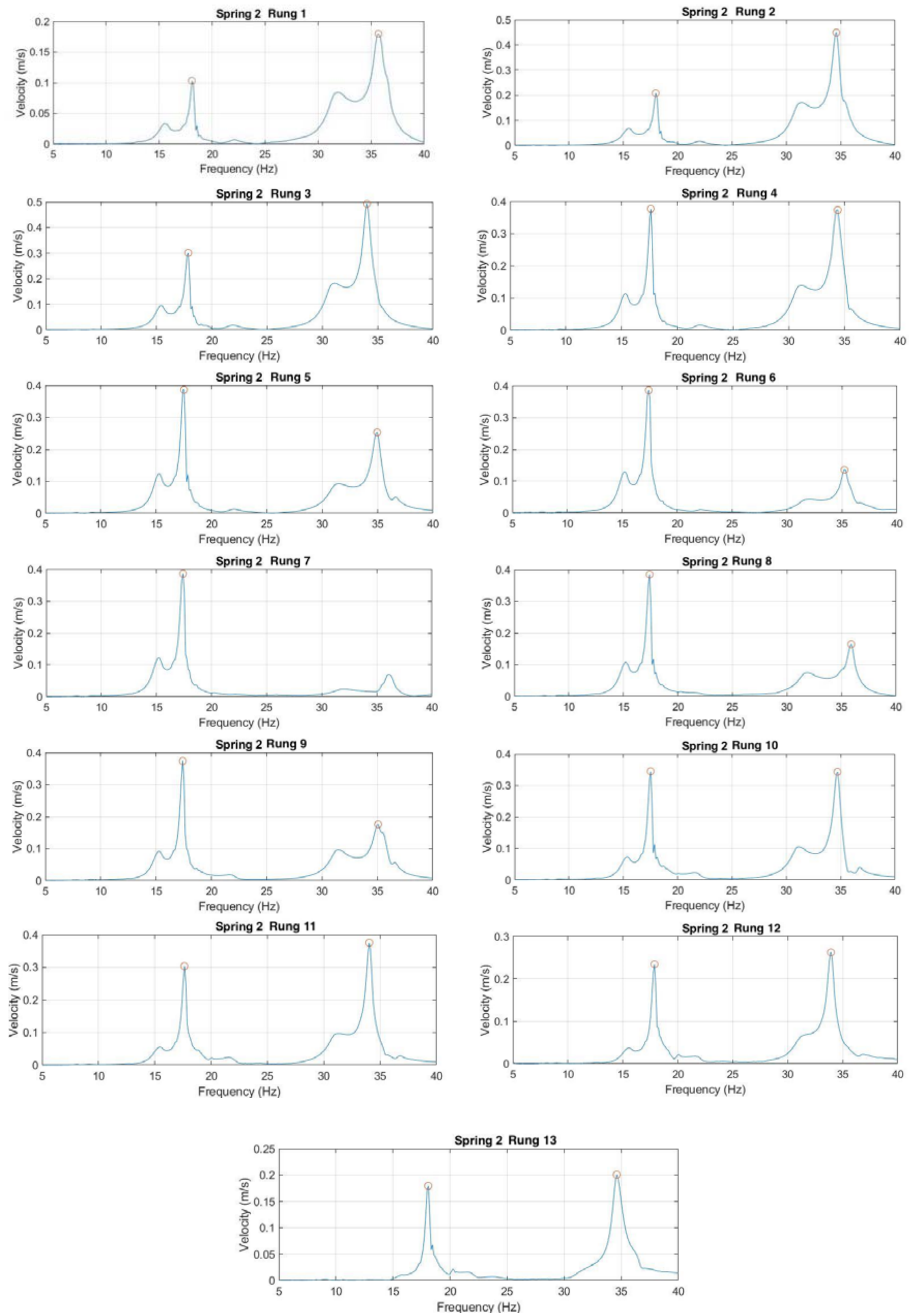

Figure 16: Spectra of data taken at each coil in CW TE-TE study

FEM Simulation Frequencies (Hz)	CW Study LE-LE Results (Hz)	Difference (%)	CW Study TE-TE Results (Hz)	Difference (%)
7.87	----	----	----	----
16.11	15.3	5.0	15.5	3.9
18.48	17.9	3.1	17.9	3.1
19.98	20.0	0.1	20.0	0.1
32.01	31.0	3.2	31.2	2.5
35.68	33.0	7.5	33.9	5.0
36.82	36.4	1.1	36.8	0.1

Table 3: Comparison of FEM simulation to CW study results

Table 3 shows the data found in the CW study and compares it to the FEM simulation frequencies. As shown, it is clear that the FEM simulation accurately reflects what was found in the initial study of Sample 2 with the highest difference found to be 7.5%. The CW study was not able to identify the mode at 7.87 Hz; however, this could be due to the amplitude of this mode being too small as compared to the amplitudes of the other modes. The TE-TE showed better results with the largest difference to be 5.0%.

It is speculated that there is a systematic difference between the measured and theoretical frequencies found. It can be seen that all modes found were measured at a higher frequency than the expected, except for the longitudinal mode expected to be found at 32.01 Hz. This could be due to some warping experienced by the helix changing its characteristics slightly offering higher modal frequencies. Damping from the continuous wave frequency sweep could also be the cause for this error.

Impulse Results

LE-LE

Figures 17 and 18 show the helix spectrum of the impulsive LE-LE study. In Figure 16, three large peaks are prominent at 14.83, 30.55, and 46.22 Hz. The mode at 46.22 Hz was not originally found in the FEM eigenfrequency study because it is not one of the first ten modes found. Figure 18 shows smaller peaks at 7.80, 16.75, 19.80, and 34.53 Hz. Each of these correspond to one of the modes found in the simulation study. Figure 19 shows the spectra taken coil by coil.

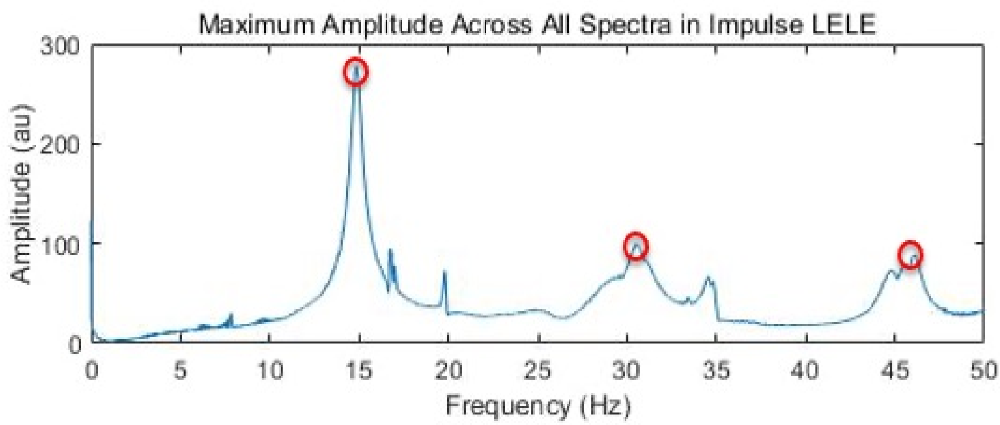

Figure 17: Figure of large peaks found in Impulse LE-LE Study

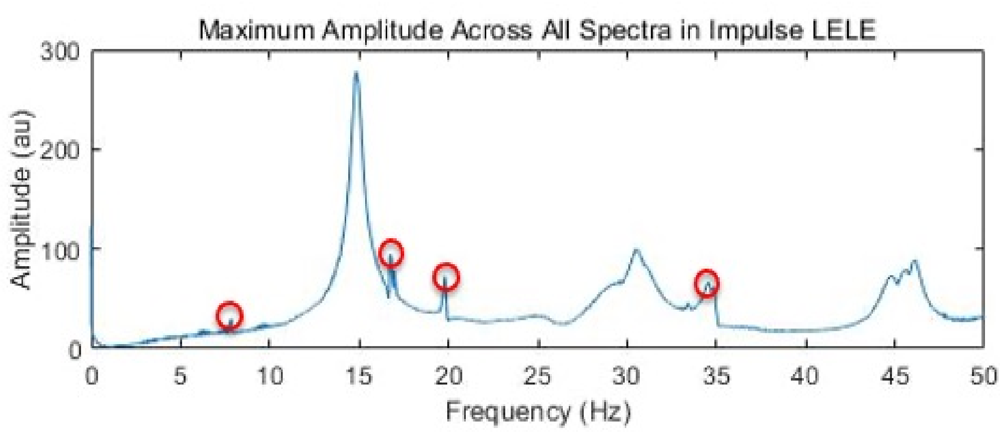

Figure 18: Image of small peaks found in Impulse LE-LE Study

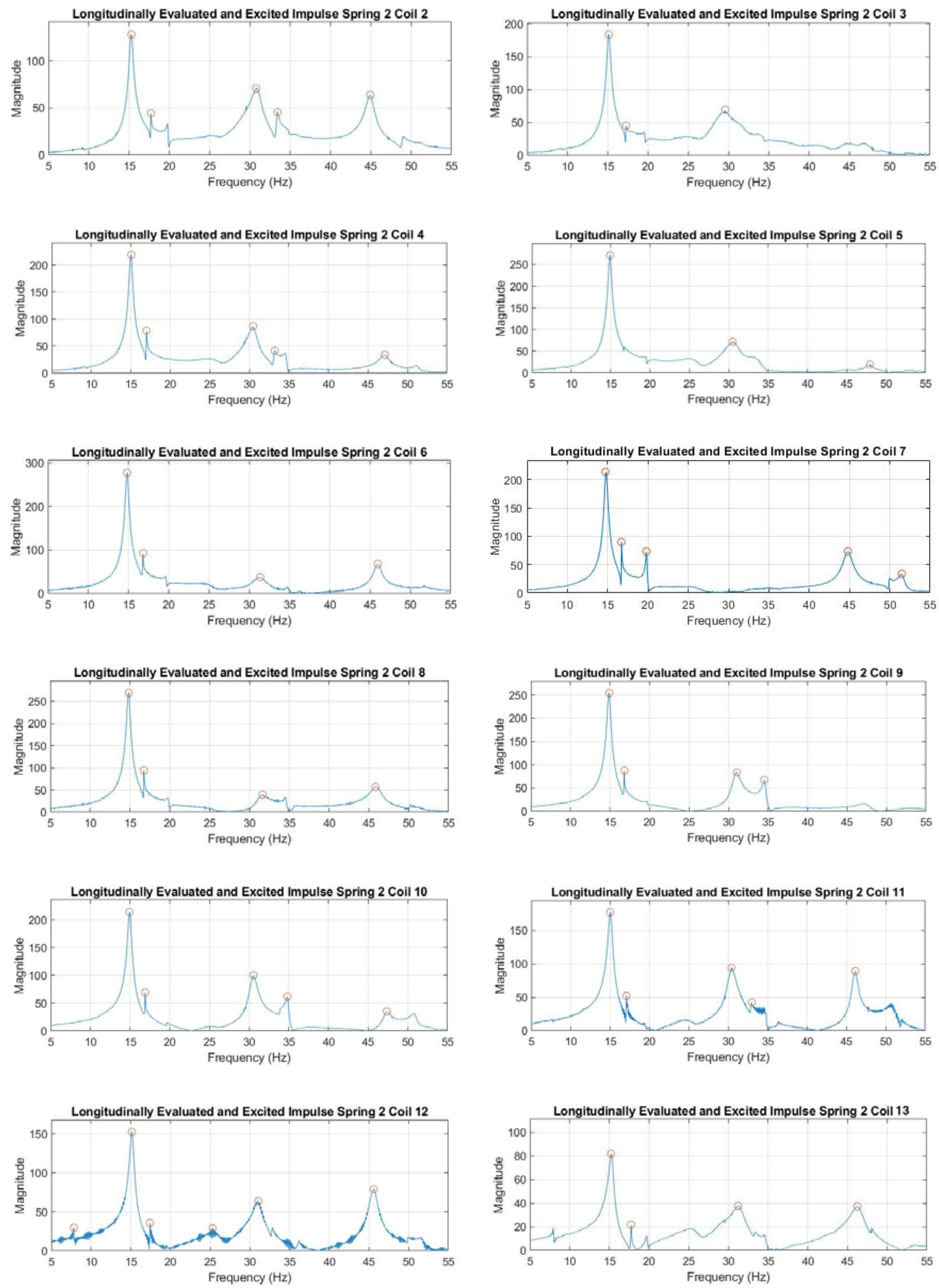

Figure 19: Spectra of Data taken at each coil in Impulse LE-LE study

LE-TE

Figure 20 shows the spectrum across the entire helix. This figure displays most modes with peaks at 8.02, 15.51, 17.56, 20.16, 30.71, 35.27 Hz. Another peak near 46.47 Hz is apparent, but this mode was not found in the original FEM study. Figure 21 shows the spectrum of each coil.

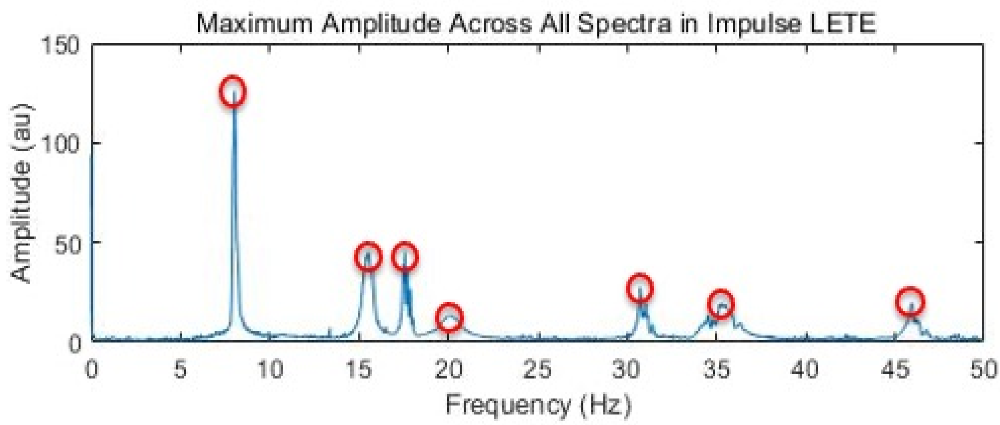

Figure 20: Figure of peaks found in Impulse LE-TE study

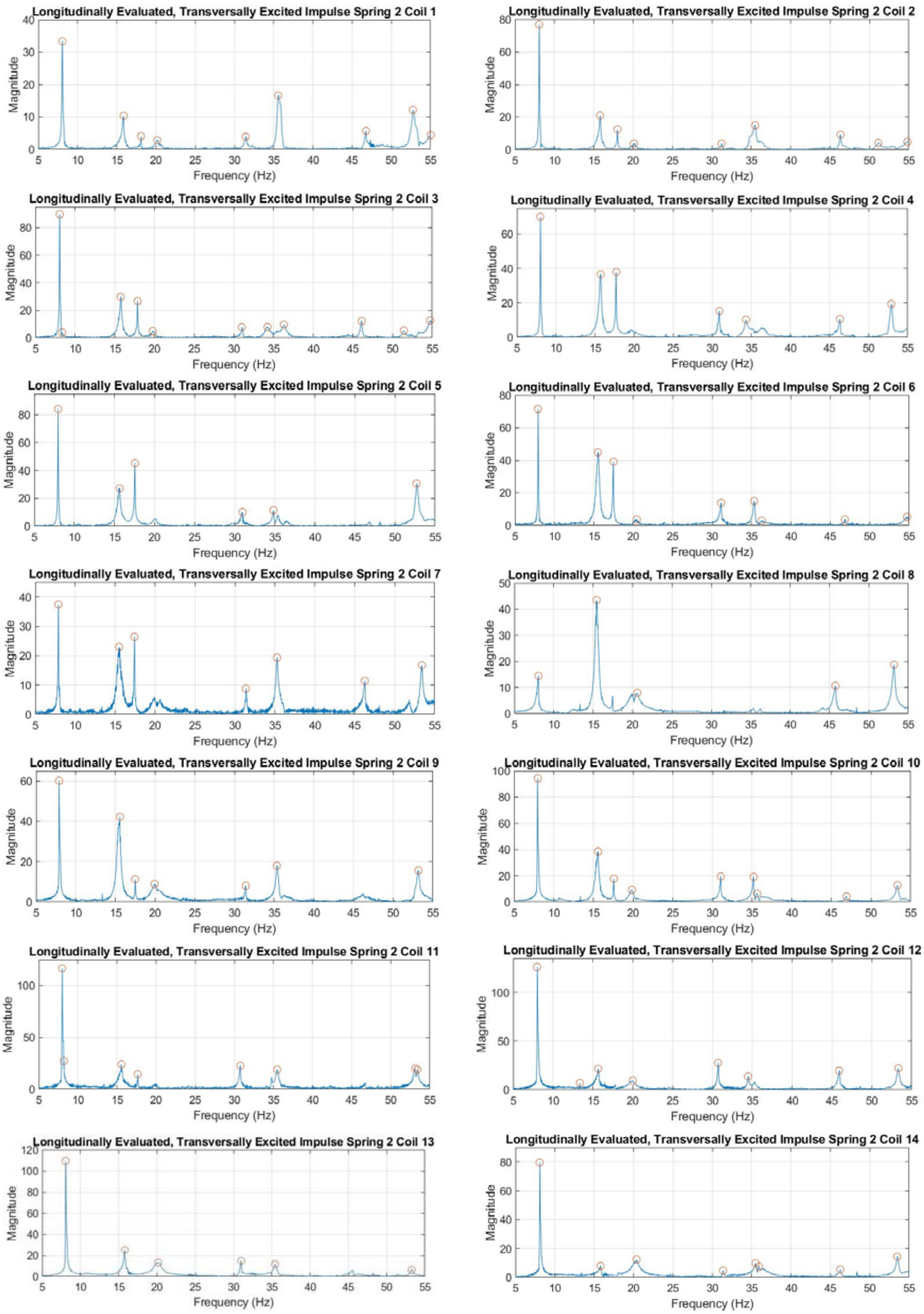

Figure 21: Spectra of data taken at each coil in Impulse LE-TE study

TE-TE

Figure 22 shows the spectrum of the helix with peaks at 8.09, 17.62, 20.00, 34.76 Hz. This accounts for every mode except for the longitudinal modes and the 36.82 Hz torsional mode. Figure 23 shows the spectrum acquired at each coil.

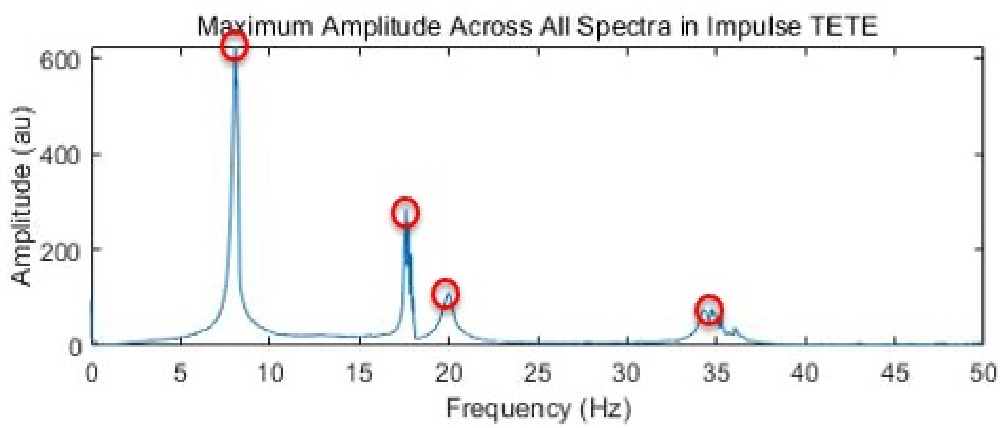

Figure 22: Figure of peaks found in Impulse TE-TE study

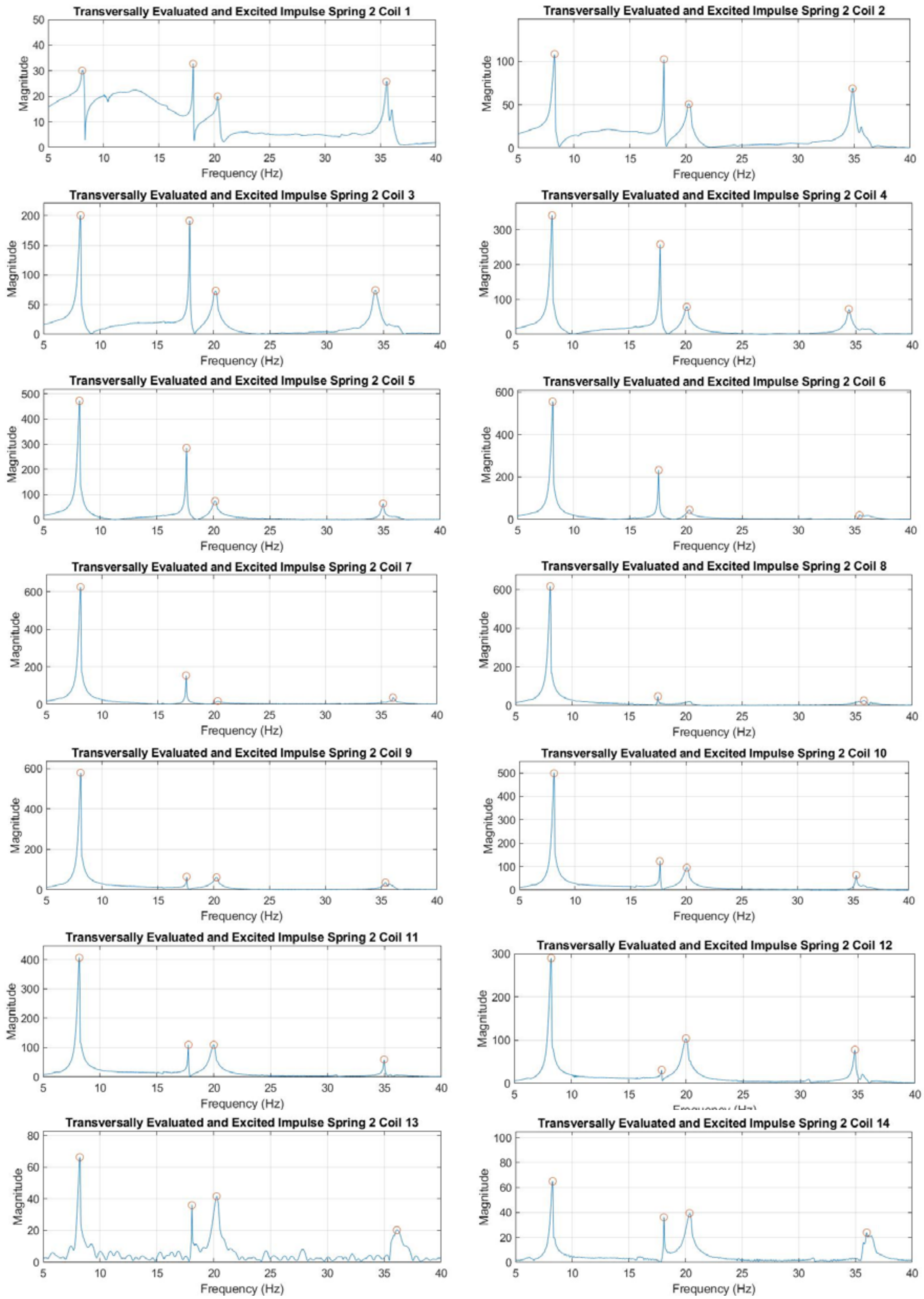

Figure 23: Spectra of data taken in Impulse TE-TE study

FEM Simulation Frequencies (Hz)	Impulse Study LE-LE Results (Hz)	Difference (%)	Impulse Study TE-TE Results (Hz)	Difference (%)
7.87	7.80	0.1	8.1	2.9
16.11	14.8	8.1	----	----
18.48	16.8	9.1	17.6	4.8
19.98	19.8	0.1	20.0	0.10
32.01	30.6	4.4	----	----
35.68	34.5	3.3	34.8	2.5
36.32	----	----	----	----

Table 4: Comparison of FEM simulation to Impulse LE-LE and TE-TE

Table 4 presents the data found in the impulse study and compares it to the FEM simulation frequencies. As shown, it is clear that the FEM simulation accurately reflects what was found in the initial study of Sample 2 with the highest difference found to be only 9.36% in the LE-LE study and 4.65% in the TE-TE study. The impulse study was not able to identify the mode at 36.32 Hz; however, this could be due to the amplitude of this mode being too small when compared to the amplitudes of the other modes. It is also possible that the mode shape caused motion that was not picked up by the LDV. The TE-TE study did not successfully find the modes at 16.12 or 32.01 Hz. This was not unexpected due to these modes being longitudinal and the TE-TE study excites the transverse modes as well as captures the amplitude and velocity of the motion in the transverse plane.

FEM Simulation Frequencies (Hz)	***Impulse Study LE-TE Results (Hz)***	***Difference (%)***
7.87	8.0	1.7
16.11	15.5	3.8
18.48	17.6	4.8
19.98	20.2	1.1
32.01	30.7	4.1
35.68	35.3	1.1
36.32	----	----

Table 5: Comparison of FEM simulation to Impulse LE-TE Results

Table 5 presents the comparison between the FEM simulation and the impulse LE-TE results. It is clear that this method provided the closest resemblance of the expected modes as it found all modes but one, with percent differences less than 5.0%. The missing mode was a torsional on predicted to be at 36.32 Hz. By tracking the amplitudes shown in Figure 20, the nodes and antinodes can be found. For example, the 30.71 Hz mode found is a first order longitudinal mode, so it is expected to have a node near the middle of the helix and antinodes on either side. This can be seen visually in the spectra. The figure shows a node is found near coil 8 with antinodes at coils 4 and 12.

Interestingly, it can be seen that the modes found in the transversally excited data during the impulse study that the majority of transverse modes were found to be at higher frequencies than the expected. Whereas the longitudinal modes in each configuration were found to be at a lower frequency than expected. This could be due to the damping created by the system or the slight changes in shape experienced by the helix after being subject to many tests.

CONCLUSION

This project consisted of several phases. The first introduced a FEM simulation of five helical samples that had been constructed for testing. Once this was done the project moved to Phase Two, consisting of a characterization of each sample utilizing LDV measurements. This characterization involved a frequency sweep from 1-20 Hz in order to understand how each helix would react under physical stimulation. One sample, (Sample 2) was chosen to continue with more extensive quantitative characterization. Phase 3 included two separate stages of testing. The first stage involved continuous wave frequency sweeps utilizing the LE-LE and TE-TE configurations. This CW study provided similar results to the COMSOL FEM study. When compared with the FEM simulation, the results showed differences with a maximum of 7.5% for all modes found. This study was unable to identify the mode at 7.87 Hz in both the LE-LE and TE-TE configurations.

The second stage involved impulsive measurements utilizing all three configurations discussed in earlier sections. Each method offered similar results to the FEM, with LE-TE offering the best results for comparison. This method displayed every mode except the 36.82 Hz torsional mode with the largest difference being only 5.0%. The TE-TE method successfully identified the transverse and torsional modes but was unsuccessful in measuring the longitudinal modes. On the other hand, LE-LE was successful in finding all but one mode.

ONGOING RESEARCH

The next phase of the project will involve finding an appropriate and effective method of damping the vibrations. The project will continue by first covering a flexible sheath around the helix to offer damping by absorbing the vibrations. Next, a boom rod will be implemented through the center to allow for more stability. The project will also begin testing the motion of the helix when not fixed to a boundary, allowing it to move freely, only influenced by the stimulus and gravity.

The next step of the project will involve rapid heating of the helix. Because the purpose of the project is proper testing of the helical structure with the knowledge this structure is to be used as an antenna for satellite communications, it is important to understand how the vibrational characteristics of the helix change when it is subject to rapid dramatic heating and cooling. This heating will mimic the absorption of radiant energy from the sun which will manifest itself in the dramatic heating and cooling cycles when the satellite passes in and out of the Earth's shadow.

REFERENCES

Wild, Flint. "What Is An Orbit?". *NASA*, 2017, <https://www.nasa.gov/audience/forstudents/5-8/features/nasa-knows/what-is-orbit-58.html.>

http://kejian1.cmatc.cn/vod/comet/satmet/satfc_j_course/orbits/navmenu.php_tab_1_page_5_0_0_type_flash.htm

Figure 1 was taken from this work

https://www.polytec.com/int/vibrometry/technology/laser-doppler-vibrometry

Equations of interferometry taken from this work

Serway, Raymond; Jewett, John, "Physics for Scientists and Engineers with Modern Physics". Physics and Astronomy, 2014

Derivation of Forced Harmonic Oscillator was adapted from this work